Theory of the Helix-Sense Inversion in Polypeptides

Hirokazu Toriumi

Department of Polymer Science, Tokyo Institute of Technology, 2-12-1 Ookayama, Meguro-ku, Tokyo 152, Japan. *Received September 28, 1983*

ABSTRACT: A theory of the helix-sense inversion in synthetic homopolypeptides is presented. By assuming that each peptide residue can interconvert its conformational state between right- and left-handed helical states and a random coil state, a statistical weight matrix representing interactions between four consecutive residues is constructed. The elimination of unfavorable conformers and redundant matrix elements reduces the order of this matrix to 9 × 9. The partition function of the entire chain is then evaluated in terms of five eigenvalues of the 9 × 9 matrix and used to obtain explicit expressions for average fractions of helical conformers. Numerical calculations reproduce fundamental aspects of experimentally observed helix-sense inversion and subsequent helix–coil transition. Variations in each conformer's fractions are discussed showing that the inversion proceeds as a result of a competition between tendencies to form right- and left-handed helices from coil residues.

I. Introduction

The statistical mechanical theory of Zimm and Bragg[1] describes the helix–coil transition in synthetic polypeptides in terms of a one-dimensional cooperative phenomenon. They assume a predominant role of intramolecular hydrogen bonds in the stabilization of an α-helix; accordingly each peptide residue in the chain is distinguished into two types by whether it is hydrogen-bonded or not. The contribution of each peptide residue to the partition function of the entire chain is calculated by a matrix method; if only the nearest-neighbor interactions are considered, this calculation can be performed with a simple 2 × 2 matrix concerned with two independent parameters, namely, an equilibrium constant S and a cooperative parameter σ of the helix formation. The original model of Zimm and Bragg has been subsequently developed by many authors to obtain its exact solution[2-6] and, on the other hand, to obtain formulas applicable to the analysis of experimental observations.[7-10]

There are, however, reported certain polypeptides that exhibit an eventful transition beyond the Zimm–Bragg model. Poly(β-phenethyl L-aspartate) (PPELA) (phenethyl group = $CH_2CH_2C_6H_5$), being in a right-handed α-helical form (RH α) in chloroform, undergoes a transition to a left-handed α-helical form (LH α) when a small amount of denaturing solvents, e.g., dichloroacetic acid (DCA) and trifluoroacetic acid (TFA), is added.[11] The LH α-helix thus formed may then be transformed into a random coil form when the acid concentration is further increased. Moreover, PPELA in an appropriate mixture of chloroform and DCA undergoes a thermally induced sense inversion from right to left upon heating. An indication of this thermally induced inversion has also been reported for poly(β-*n*-propyl L-aspartate) in chloroform.[12,13] Generally, preferred conformations of poly(L-aspartate esters) vary depending upon the nature of side chain and the solution conditions such as solvent and temperature. Bradbury et al.[12-14] and Hashimoto et al.[15,16] have suggested by examining conformational transitions in various homo- and copolymers that the stabilities of two α-helical forms of poly(L-aspartate esters) are quite small and close together.

A theory describing conformational transitions in homopoly(aspartate esters), which may undergo the helix-sense inversion as well as the helix–coil transition, must precisely represent the capability of each peptide residue to interconvert its conformational state between RH α, LH α, and random coil states. The purpose of this study is to develop a model applicable to this situation. The present model distinguishes three conformational states according to the rotational angles around two rotatable skeletal single bonds in a peptide residue and evaluates a statistical weight matrix for four consecutive residues considering the stabilization effect due to the hydrogen-bond formation.

Information on the stability differences between two α-helical forms may also be obtained by analyzing the sense inversions in copoly(aspartate esters);[12-16] however, the application of the three-state model to such systems would face a difficulty associated with the generally unspecified sequences of amino acid residues in the chain.[17] Moreover, even for regular-sequence or ideally random-sequence copolymers, the computation still remains hugh since each matrix involves different statistical weights for each amino acid residue, preventing a diagonalization of the matrix product. All such problems are eliminated in the case of homopolymers. As will be seen, the statistical weight matrix for homopolymers is given identical for all residues and involves only a minimal number of parameters. This advantage allows us to calculate various molecular averages associated with the sense inversion by using a mathematical method developed by Zimm and Bragg[1] and Nagai.[4,5] The primary goal of this paper is to describe the model and derive formulas for helix fractions that can be readily compared with experimental observations. To discuss fundamental aspects of the sense inversion, the model will also be analyzed numerically under certain typical conditions.

II. Theory

Model and Transition Matrix. Underlying the present model is a basic requirement for the hydrogen-bond formation in a polypeptide chain that only when three consecutive residues are cooperatively distorted to an α-helical state the hydrogen-bond bridge can form and stabilize this helix sequence. This requirement may be disregarded in the theory of a simple helix–coil transition (in fact, an approximated 2 × 2 matrix treatment of Zimm and Bragg works effectively to reproduce the transition curve);[1,8] however, it should be explicitly represented in the case of the helix-sense inversion to exclude the occurrence of unreasonable sequences. The Nagai model[4,5] including this long-range interaction will be followed here to develop a theory applicable to the sense inversion.

The polypeptide chain is regarded to consist of a linear array of monomeric residues (–CO–C$^\alpha$HR–NH–), with R being a side chain attached to the α-carbon atom. Then we number all residues as 1, 2, ..., N from the free carboxyl end. A hydrogen bond in this case will form between the amido hydrogen atom of a given residue (say, i – 2) and

0024-9297/84/2217-1599$01.50/0

Table I
Statistical Weight Matrix W′

			$i+1$	r	l	r	l	r	r	r	l	l	l	c	c	c	c	c
	p		q i	r	l	r	l	c	c	c	c	c	c	r	l	c	c	c
$i-2$	$i-1$	i	$i-1$	r	l	c	c	r	l	c	r	l	c	r	l	r	l	c
r	r	r		α_r										$\alpha_{r,1}$				
l	l	l			α_l										$\alpha_{l,1}$			
c	r	r		α_r														
c	l	l			α_l													
r	c	r				$\alpha_{r,2}$												
l	c	r				$\alpha_{r,2}$												
c	c	r				$\alpha_{r,2}$												
r	c	l	W′ =				$\alpha_{l,2}$											
l	c	l					$\alpha_{l,2}$											
c	c	l					$\alpha_{l,2}$											
r	r	c						$\gamma_{r,1}$			δ_1					$\gamma_{r,2}$		
l	l	c							δ_2			$\gamma_{l,1}$					$\gamma_{l,2}$	
r	c	c								$\gamma_{r,3}$			$\gamma_{l,3}$					1
l	c	c								$\gamma_{r,3}$			$\gamma_{l,3}$					1
c	c	c								$\gamma_{r,3}$			$\gamma_{l,3}$					1

the amido oxygen atom of its fourth succeeding residue ($i + 2$) when all intervening residues ($i - 1$, i, and $i + 1$) are distorted to the α-helical state. Any one of such distorted residues is called a helix unit, but here we have to distinguish two different types of the helix unit. One which has the rotational angles around the skeletal single bonds C–C$^\alpha$ and C$^\alpha$–N equal to those characteristic of the RH α conformation is defined as an r unit. The other one having the rotational angles equal to those of the LH α conformation is defined as an l unit. A residue involving any arbitrary set of the rotational angles other than the above two is called a random coil unit and denoted by a c unit.

According to the requirement that the helix sequence becomes stabilized when it involves three consecutive helix units, the occurrences of chc and chhc (h = r or l) sequences should be disregarded.[4,5] The latter sequence including four residues is the longest sequence whose interaction is to be considered; in other words, a possible state of the ith residue cannot be uniquely determined until the states of its neighboring three residues ($i - 2$, $i - 1$, and $i + 1$) are fixed. The transition matrix for the ith residue must therefore be constructed with the rows corresponding to the states of residues ($i - 2$, $i - 1$, and i) and the columns to the states of residues ($i - 1$, i, and $i + 1$). This matrix would have a size of $3^3 \times 3^3$ since each residue is assumed to adopt three different conformational states. Fortunately, some of the 27 triads can be excluded according to the aforementioned requirement and molecular model considerations. First of all, six triads of the types rlr, rlc, lrl, lrc, crl, and clr are excluded because they can not be stabilized by any hydrogen-bond bridges. Also excluded for the same reason are rllr and lrrl. If only the hydrogen-bond formation is considered, the rl contact may be allowed at a junction of r and l helices both of which involve at least three helix units

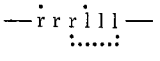

The molecular model however shows that the side-chain nonbonded interactions for pairs indicated by dotted lines become considerably large and disrupt such sequences. Triads excluded by this mechanism are rrl, rll, lrr, and llr. In short, all triads involving adjoining rl units should be omitted. Finally there remain 15 allowable triads and their statistical weights may be given as follows:

rrr	α_r	ccr	$\gamma_{r,3}$	cll	$\alpha_{l,2}$
rrc	$\alpha_{r,1}$	rcl	δ_1	lcl	$\gamma_{l,1}$
crr	$\alpha_{r,2}$	ccc	1	lcc	$\gamma_{l,2}$
rcr	$\gamma_{r,1}$	lll	α_l	ccl	$\gamma_{l,3}$
rcc	$\gamma_{r,2}$	llc	$\alpha_{l,1}$	lcr	δ_2

With these quantities a transition matrix W′ can be written as shown in Table I. The (p, q) element of W′ represents the probability of occurrence of the qth state at the ith residue in a sequence of four residues ($i - 2$, $i - 1$, i, and $i + 1$); it is obvious that each element can have a nonzero value only if the first and second symbols of the qth sequence are equal to the second and third symbols of the pth sequence, respectively, and that it becomes zero in all other cases. The (3, 11) and (4, 12) elements, which produce the prohibited chhc sequences, are taken to be zero.

The matrix W′ gives a general description of the present model. However, for the sake of an intuitive understanding of the inversion mechanism, some of detailed discussions in W′ may have to be omitted. The (6, 3) element of W′ represents the statistical weight for the r unit involved in the tightest sense-inversion process from left to right, lcrr. This weight may be different from those for the r units at the ith residue in less constrained circumstances such as rcrr, ccrr, and rrrc. However, since no information is available about the difference, we may assume an identical weight for all these four r units. A similar assumption can be applied to the l units at the i residue appearing in the fourth and twelfth columns and also to all c units. The degree of our simplification remains at a level with those discussed in previous helix–coil transition theories.[1,4,5] Under these conditions, the statistical weights are redefined as follows by using common S and σ parameters,[18]

$$\alpha_r = S_r$$
$$\alpha_l = S_l$$
$$\alpha_{r,1} = \alpha_{r,2} = \sigma_r^{1/2} \qquad (1)$$
$$\alpha_{l,1} = \alpha_{l,2} = \sigma_l^{1/2}$$
$$\gamma_{r,1} = \gamma_{r,2} = \gamma_{r,3} = \gamma_{l,1} = \gamma_{l,2} = \gamma_{l,3} = \delta_1 = \delta_2 = 1$$

The 15 × 15 matrix W′ is then condensed into a simple

9×9 matrix **W** shown in Table II. There, the notation "r $\cup$ l $\cup$ c" is used for "r, l, or c" to eliminate redundant elements.[6]

Partition Function. The partition function of a polypeptide chain consisting of N residues would be written as

$$Z_N = \mathbf{e}_1 \mathbf{W}^{N-2} \mathbf{e}_N \tag{2}$$

The end vectors associated with the first and last residues, which are assumed never to be involved in the helix section, are expressed as

$$\mathbf{e}_1 = (0, 0, 0, 0, 1, 1, 0, 0, 1) \tag{3}$$

and

$$\mathbf{e}_N = (0, 0, 0, 0, 0, 0, 1, 1, 1)^{\mathrm{T}} \tag{4}$$

where the superscript T denotes the transpose of a vector.

To evaluate eq 2, we expand **W** by its eigenvalues and eigenvectors after Nagai's prescription.[4,5] The secular equation of **W** is written as follows by omitting an eigenvalue $\lambda = 0$ with a multiplicity of four:

$$\lambda^2(\lambda - 1)(\lambda - S_r)(\lambda - S_l) - \sigma_r S_r(\lambda - S_l) - \sigma_l S_l(\lambda - S_r) = 0 \tag{5}$$

Five roots of this equation determined numerically are then denoted by λ_i (i = 1–5) in the order of magnitude. By solving the following equations concerning λ_i, we have the right-hand side and left-hand side eigenvectors denoted respectively by $\mathbf{u}(\lambda_i)$ and $\mathbf{v}(\lambda_i)$:

$$\mathbf{W}\mathbf{u}(\lambda_i) = \lambda_i \mathbf{u}(\lambda_i) \tag{6}$$

$$\mathbf{v}(\lambda_i)\mathbf{W} = \lambda_i \mathbf{v}(\lambda_i) \tag{7}$$

and

$$\mathbf{v}(\lambda_j)\mathbf{u}(\lambda_k) = \delta_{jk} \qquad (j, k = 1\text{–}5) \tag{8}$$

where δ_{jk} is Kronecker's δ. The **u** and **v** eigenvectors for $\lambda = \lambda_1, \lambda_2, \ldots, \lambda_5$ expressed in the normalized form are

$$\mathbf{u}(\lambda) = \left(1, \frac{\sigma_l^{1/2}}{\sigma_r^{1/2}} \frac{\lambda - S_r}{\lambda - S_l}, \frac{S_r}{\lambda}, \frac{\sigma_l^{1/2} S_l}{\sigma_r^{1/2}} \frac{\lambda - S_r}{\lambda - S_l} \frac{1}{\lambda}, \frac{\sigma_r^{1/2} S_r}{\lambda^2}, \frac{\sigma_l S_l}{\sigma_r^{1/2}} \frac{\lambda - S_r}{\lambda - S_l} \frac{1}{\lambda^2}, \frac{\lambda - S_r}{\sigma_r^{1/2}}, \frac{\lambda - S_r}{\sigma_r^{1/2}}, \frac{\lambda - S_r}{\sigma_r^{1/2}} \right)^{\mathrm{T}} \tag{9}$$

and

$$\mathbf{v}(\lambda) = C(\lambda) \left(1, \frac{\sigma_l^{1/2} S_l}{\sigma_r^{1/2} S_r} \frac{\lambda - S_r}{\lambda - S_l}, \frac{\lambda - S_r}{S_r}, \frac{\sigma_l^{1/2}(\lambda - S_r)}{\sigma_r^{1/2} S_r}, \frac{\lambda(\lambda - S_r)}{\sigma_r^{1/2} S_r}, \frac{\lambda(\lambda - S_r)}{\sigma_r^{1/2} S_r}, \frac{\sigma_r^{1/2}}{\lambda}, \frac{\sigma_l S_l}{\sigma_r^{1/2} S_r} \frac{\lambda - S_r}{\lambda - S_l} \frac{1}{\lambda}, \frac{\lambda(\lambda - S_r)}{\sigma_r^{1/2} S_r} \right) \tag{10}$$

where

$$C(\lambda) = \sigma_r^2 S_r \frac{\lambda - S_l}{\lambda - S_r} F(\lambda) \tag{11}$$

$$F(\lambda) = \{5\lambda^4 - 4(S_r + S_l + 1)\lambda^3 + 3(S_r + S_l + S_r S_l)\lambda^2 - 2S_r S_l \lambda - (\sigma_r S_r + \sigma_l S_l)\}^{-1} \tag{12}$$

Then the matrix **W** can be expanded as

$$\mathbf{W} = \sum_{\lambda} \lambda \mathbf{u}(\lambda)\mathbf{v}(\lambda) \tag{13}$$

Hence

$$\mathbf{W}^{N-2} = \sum_{\lambda} \lambda^{N-2} \mathbf{u}(\lambda)\mathbf{v}(\lambda) \tag{14}$$

Finally, by combining eq 2–4, 9–12, and 14, we have

$$Z_N = \sum_{\lambda} \lambda^{N-2} \mathbf{e}_1 \mathbf{u}(\lambda)\mathbf{v}(\lambda)\mathbf{e}_N = \sum_{\lambda} \lambda^{N+1}(\lambda - S_r)(\lambda - S_l)F(\lambda) \tag{15}$$

Fractions of r and l Units. The occurrence of the r state at the ith residue is represented in the matrix **W** as three different types of joint conformations—rrr with a statistical weight S_r, rrc with $\sigma_r^{1/2}$, and crr with $\sigma_r^{1/2}$—so that the average number of the r units in the entire chain can be calculated as a sum of powers of S_r and $\sigma_r^{1/2}$ in Z_N. Considering again that two residues at chain ends can not adopt the helical states, we obtain the average fraction of the r unit, f_r, as follows:

$$f_r = \frac{1}{N-2}\left(\frac{\partial \ln Z_N}{\partial \ln S_r} + \frac{\partial \ln Z_N}{\partial \ln \sigma_r^{1/2}} \right) = \frac{1}{(N-2)Z_N} \sum_{\lambda} \lambda^N \{N(\lambda - S_r)(\lambda - S_l)(3\lambda - 2S_r)A_l(\lambda)F^2(\lambda) - I_r(\lambda)\} \tag{16}$$

where

$$I_r(\lambda) = [\lambda(\lambda - S_r)(\lambda - S_l)(3\lambda - 2S_r)A_l(\lambda)B(\lambda)F(\lambda) + \lambda(\lambda - S_l)(3\lambda - 2S_r)A_r(\lambda) - \{(3\lambda - 2S_r)(2\lambda - S_l) + 3\lambda(\lambda - S_l)\}(\lambda - S_r)A_l(\lambda) - \lambda^3(\lambda - 1)(\lambda - S_r)(\lambda - S_l)(3\lambda - 2S_r)]F^2(\lambda) \tag{17}$$

$$A_r(\lambda) = \lambda^2(\lambda - 1)(\lambda - S_r) - \sigma_r S_r \tag{18}$$

$$A_l(\lambda) = \lambda^2(\lambda - 1)(\lambda - S_l) - \sigma_l S_l \tag{19}$$

and

$$B(\lambda) = 20\lambda^3 - 12(S_r + S_l + 1)\lambda^2 + 6(S_r + S_l + S_r S_l)\lambda - 2S_r S_l \tag{20}$$

with $\lambda = \lambda_1, \lambda_2, \ldots, \lambda_5$. The average fraction of the l unit, f_l, can be calculated in a similar way:

$$f_l = \frac{1}{N-2}\left(\frac{\partial \ln Z_N}{\partial \ln S_l} + \frac{\partial \ln Z_N}{\partial \ln \sigma_l^{1/2}} \right) = \frac{1}{(N-2)Z_N} \sum_{\lambda} \lambda^N \{N(\lambda - S_r)(\lambda - S_l)(3\lambda - 2S_l)A_r(\lambda)F^2(\lambda) - I_l(\lambda)\} \tag{21}$$

where

$$I_l(\lambda) = [\lambda(\lambda - S_r)(\lambda - S_l)(3\lambda - 2S_l)A_r(\lambda)B(\lambda)F(\lambda) + \lambda(\lambda - S_r)(3\lambda - 2S_l)A_l(\lambda) - \{(3\lambda - 2S_l)(2\lambda - S_r) + 3\lambda(\lambda - S_r)\}(\lambda - S_l)A_r(\lambda) - \lambda^3(\lambda - 1)(\lambda - S_r)(\lambda - S_l)(3\lambda - 2S_l)]F^2(\lambda) \tag{22}$$

Conventional polarimetric measurements cannot determine f_r and f_l separately but measure their difference, $f_r - f_l$. From eq 16 and 21, an equation for the latter quantity is given as

$$f_r - f_l = \frac{1}{(N-2)Z_N} \sum_{\lambda} \lambda^N \{N(\lambda - S_r)(\lambda - S_l)A(\lambda)F^2(\lambda) - I(\lambda)\} \tag{23}$$

where

$$A(\lambda) = (3\lambda - 2S_r)A_l(\lambda) - (3\lambda - 2S_l)A_r(\lambda) \tag{24}$$

and

$$I(\lambda) = I_r(\lambda) - I_l(\lambda) \tag{25}$$

Table II
Condensed Statistical Weight Matrix W

p			$i+1$	r	l	r	l	r	l	c	c	c
			q i	r	l	r	l	c	c	r	l	c
$i-2$	$i-1$	i	$i-1$	r	l	c	c	r∪l∪c	r∪l∪c	r	l	r∪l∪c
r	r	r		S_r						$\sigma_r^{1/2}$		
l	l	l			S_l						$\sigma_l^{1/2}$	
c	r	r		S_r								
c	l	l			S_l							
r∪l∪c	c	r	W =			$\sigma_r^{1/2}$						
r∪l∪c	c	l					$\sigma_l^{1/2}$					
r	r	c						1	1			1
l	l	c						1	1			1
r∪l∪c	c	c						1	1			1

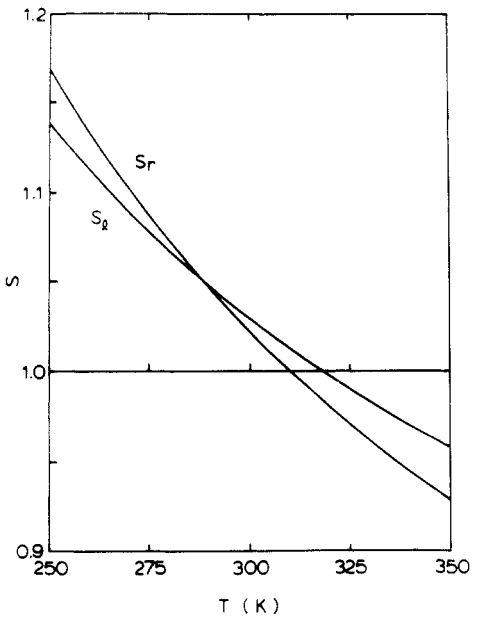

Figure 1. Temperature dependence of the equilibrium constant S for $\Delta H_r = -400$ cal/mol, $T_r = 310$ K, $\Delta H_l = -300$ cal/mol, and $T_l = 318$ K.

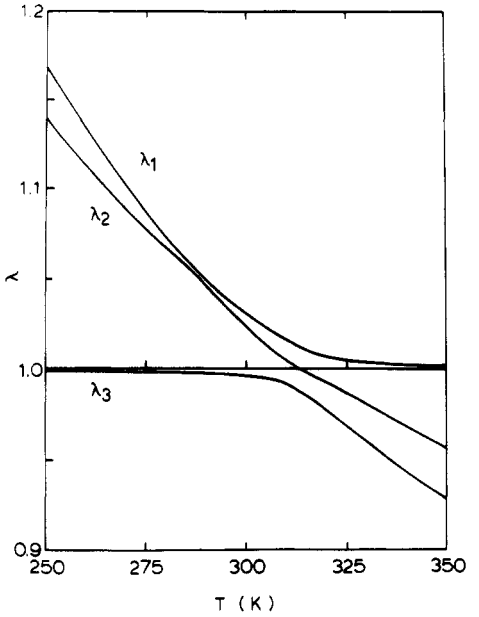

Figure 2. Three major eigenvalues of matrix **W** calculated with the parameters given in Figure 1.

When N is sufficiently large and λ_i^N (i = 2–5) can be ignored compared with λ_1^N, an asymptotic form of $f_r - f_l$ becomes

$$f_r - f_l = \frac{A(\lambda_1)F(\lambda_1)}{\lambda_1} + \frac{1}{N}\left\{\frac{2A(\lambda_1)F(\lambda_1)}{\lambda_1} - \frac{I(\lambda_1)}{\lambda_1(\lambda_1 - S_r)(\lambda_1 - S_l)F(\lambda_1)}\right\} \quad (26)$$

Further, for infinitely large N, we have

$$f_r - f_l = \frac{A(\lambda_1)F(\lambda_1)}{\lambda_1} \quad (27)$$

III. Results and Discussion

Equilibrium Constants and Major Eigenvalues. To perform numerical analyses of thermally induced conformational transitions, we express the equilibrium constant of the helix formation S as a function of the absolute temperature T. According to a normal thermodynamic definition

$$S_h = \exp\{-(\Delta H_h/RT)(1 - T/T_h)\} \quad (h = r, l) \quad (28)$$

where ΔH_h is the enthalpy change associated with the helix–coil transition occurring at T_h and R is the gas constant. Both the helix-sense inversion and the subsequent helix–coil transition can be expected to occur in a particular range of temperature when the T_h values are chosen appropriately. Here we assume $T_r = 310$ K, $T_l = 318$ K, and a midpoint of the sense inversion at 288.2 K (more precisely this represents a temperature at which S_r becomes equal to S_l). These characteristic temperatures will determine the ratio $\Delta H_r/\Delta H_l = {}^4/_3$, yet either one of ΔH's has to be determined. We adopt $\Delta H_l = -300$ cal/mol as an example, hence $\Delta H_r = -400$ cal/mol, and discuss later the influence of their magnitudes on the transition profile. The negative ΔH values represent that both helical conformers undergo a "normal transition"; i.e., the change proceeds from helix to coil with increasing temperature. For a simplification, the σ values are assumed to be temperature independent and identical for both r and l conformers; $\sigma_r = \sigma_l = 5 \times 10^{-5}$.

Figures 1 and 2 illustrate the temperature dependences of equilibrium constants and those of three major eigenvalues calculated for the parameters given above, respectively. We find by comparing two figures that λ_1, λ_2, and λ_3 adopt values being, although not exactly the same, close to S_r, S_l, and unity arranged in order of magnitude, respectively (the value of unity can be regarded as an equilibrium constant for the coil formation). The largest

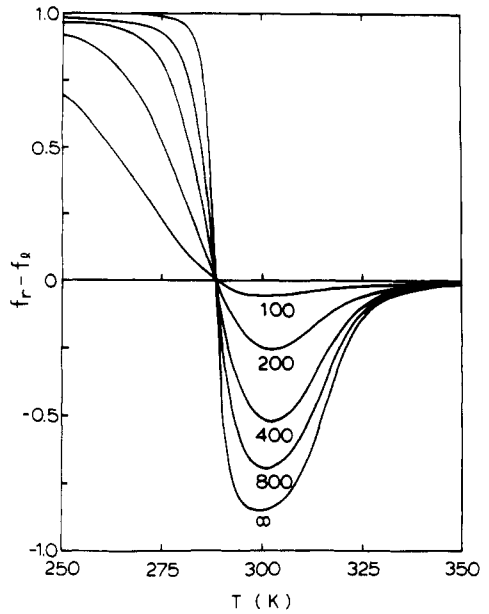

Figure 3. N dependence of the $f_r - f_l$ vs. T curve for $\Delta H_r = -400$ cal/mol, $T_r = 310$ K, $\Delta H_l = -300$ cal/mol, $T_l = 318$ K, and $\sigma_r = \sigma_l = 5 \times 10^{-5}$.

eigenvalue λ_1, which makes a predominant contribution in determining the favorable conformation of the chain, samples S_r, S_l, and then unity as temperature is increased; hence this chain is expected to undergo an RH $\alpha \rightarrow$ LH $\alpha \rightarrow$ random coil transition upon heating. If the chain is sufficiently long so that $\lambda_1^N \gg \lambda_i^N$ ($i = 2$–5), λ_1 by itself can determine the fractions of three conformers in equilibrium; however, for shorter chains contributions of λ_2 and λ_3 cannot be ignored. These contributions are especially important in the transition region around 300 K, where λ_2 and λ_3 become large comparable to λ_1; e.g., the ratio λ_2/λ_1 runs up to 0.998 at 288 K. On the other hand, the remaining two eigenvalues (λ_4 and λ_5) stay always on the order of 10^{-2} (not shown) and make only minor contributions even when the chain is quite short.

It should be noted here that the present theory calculates three major eigenvalues differing from preceding theories of a simple helix–coil transition which involve only two major eigenvalues.[1-7] This difference arises as a consequence that we have introduced the second helical state into conventional helix–coil equilibrium. As should be expected, if we ignore the occurrence of this additional helical conformer, all our formulas reduce to those developed in the previous theories. For example, by putting $S_l = 0$, eq 5 reduces to a quartic equation (the eigenvalue corresponding to λ_2 vanishes in the temperature range below 288.2 K), the equation of f_r in eq 16 reduces to that in eq 42 of ref 5, and f_l in our eq 21 becomes zero.

Transition Curves and Helix Fractions. The transition curve, $f_r - f_l$ vs. T, is calculated in Figure 3 as a function of N. The RH $\alpha \rightarrow$ LH α transition is unique in that the curves for different N intersect with each other at $f_r - f_l = 0$ and $T = 288.2$ K; note the latter is the temperature at which $S_r = S_l$. This characteristic should provide a simple means to eliminate one adjustable parameter when the theory is applied to the analysis of experimental observations. The negative trough and the right-hand side midpoint of the $f_r - f_l$ curve are also found in a very narrow range of temperature. The absolute value of $f_r - f_l$ increases at any given temperature as N is increased; consequently the transition curve becomes sharper for a longer chain. The most conspicuous effect of N is seen in the depth of the trough around 300 K, which changes as much as from 0.06 at $N = 100$ to 0.85 at $N = \infty$.

To show this effect of N clearer, the temperature dependences of f_r and f_l are separately illustrated in Figure 4. First of all, it should be noted that the f_l curve takes a convex shape in contrast with a simple sigmoidal curve of f_r. The initial increase in f_l and the corresponding decrease in f_r are associated with the LH α-helix formation proceeding at the expense of the RH α-helix, and the decrease in f_l at higher temperatures represents a melting of the LH α-helix into the random coil form. The peak temperature of the f_l curve shifts markedly to higher values with N; however, as seen in Figure 3 the negative trough of the $f_r - f_l$ curve maintains its position within a narrow temperature range around 300 K. It follows therefore that the depth of the latter curve, although being experimentally referred to as an LH α content, does not directly represent the maximum f_l value. This discrepancy arises from a considerable coexistence of the RH α-helix in the LH α region; for example, at $T = 302$ K and $N = 200$, the f_r and f_l values are found to be 0.161 and 0.416, respectively; hence the depth of the $f_r - f_l$ curve reproduces only 60% of the true LH α content. A similar discrepancy appears also in the midpoint of the LH $\alpha \rightarrow$ coil transition. Such being the case, the conformer's fractions or the transition parameters cannot be directly evaluated from experimentally observed $f_r - f_l$ data. A curve-fitting method is so far the only one available method to estimate these quantities, where as noted above the calculation can be simplified to a certain extent by the peculiarity of the RH $\alpha \rightarrow$ LH α crossover point.

Also included in Figure 4 is a total helix fraction, $f_r + f_l$, from which a coil fraction can be calculated as $1 - (f_r + f_l)$. It is clearly seen that the $f_r + f_l$ curve exhibits only a monotonous decrease in the entire range of temperature. The absence of a hollow from this curve in the sense-inversion region may indicate an inversion mechanism which does not necessarily involve the formation of respectably long coil sequences. This suggestion is further corroborated by the result in Figure 1 that S_r and S_l remain always greater than unity in the inversion region, making the coil conformer less favorable than the RH and LH α-helices. The sense inversion is therefore expected to proceed in such a manner as to propagate a center of inversion successively along the chain. The viscosity curve observed for PPELA[11] shows a temperature dependence resembling that seen in the $f_r + f_l$ curve.

Figure 5 shows transition curves calculated for different sets of ΔH_r and ΔH_l. Since the $\Delta H_r/\Delta H_l$ ratio is kept constant, the increase in ΔH_r (or ΔH_l) simply expands a difference between S_r and S_l according to eq 28 without influencing the characteristic temperature of the sense inversion. Changes in the absolute $f_r - f_l$ value and in the transition sharpness with ΔH appear in a similar manner as observed when N is increased in Figure 3 (note that the fraction of the most favorable conformer increases as $(\lambda_1/\lambda_i)^N$ ($i = 2$–5) is increased by changing either N or the difference in the equilibrium constant). Only a slight difference between the effects of N and ΔH is seen in the sharpness of the LH $\alpha \rightarrow$ coil transition tail at high temperatures.

Sense Inversion with Inverse Helix–Coil Transition. The direction of the helix–coil transition may vary depending upon solvent. Hayashi et al.[19] have shown for poly(β-benzyl L-aspartate) (PBLA) that the transition in m-cresol proceeds from helix to coil upon heating (normal transition), while that in chloroform–DCA mixed solvents proceeds from coil to helix (inverse transition). Mathe-

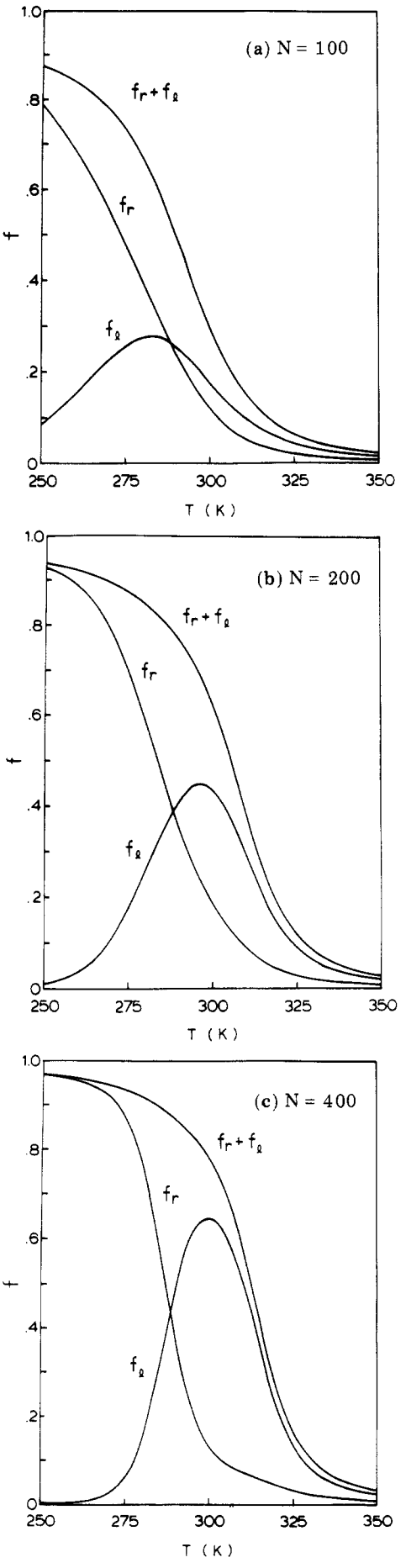

Figure 4. Curves of f_r, f_l, and $f_r + f_l$ vs. T at (a) $N = 100$, (b) 200, and (c) 400.

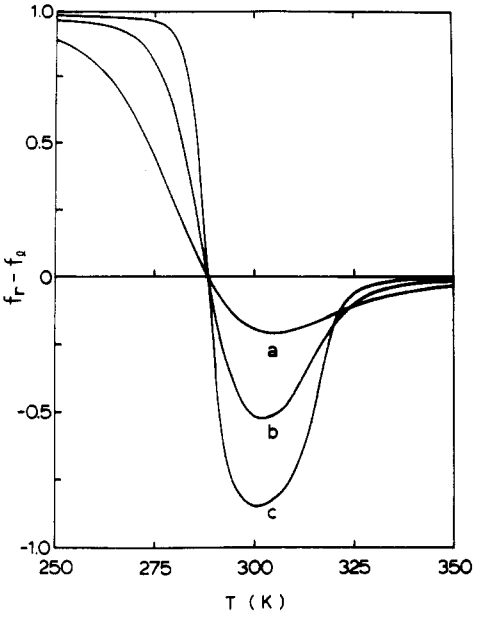

Figure 5. Effect of ΔH on the $f_r - f_l$ curve at $\sigma_r = \sigma_l = 5 \times 10^{-5}$ and $N = 400$: (a) $\Delta H_r = -200$ cal/mol, $\Delta H_l = -150$ cal/mol; (b) $\Delta H_r = -400$ cal/mol, $\Delta H_l = -300$ cal/mol; (c) $\Delta H_r = -800$ cal/mol, $\Delta H_l = -600$ cal/mol.

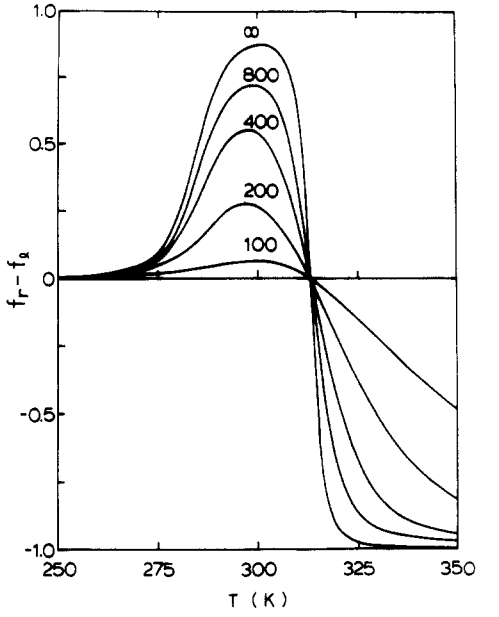

Figure 6. N dependence of the $f_r - f_l$ vs. T curve in a system involving the inverse helix–coil transition. Parameters are $\Delta H_r = 300$ cal/mol, $T_r = 283$ K, $\Delta H_l = 400$ cal/mol, $T_l = 290$ K, and $\sigma_r = \sigma_l = 5 \times 10^{-5}$.

matically these two courses are distinguished by the sign of ΔH in eq 28; a positive sign is identified with the inverse transition. Unfortunately, our experiment for PPELA in chloroform–DCA has failed to determine the direction of the helix–coil transition associated with the sense inversion.[11] The coil formation, expected around 5–7% DCA content in analogy with PBLA data,[19] is hidden by the polymer precipitation occurring at ~5% DCA. To demonstrate how the RH → LH sense inversion occurs if the system involves the inverse helix–coil transition instead of the normal one, Figure 6 illustrates examples of the $f_r - f_l$ curve. Parameters employed are $\Delta H_r = 300$ cal/mol, $T_r = 283$ K, $\Delta H_l = 400$ cal/mol, $T_l = 290$ K, and $\sigma_r = \sigma_l = 5 \times 10^{-5}$, which determine the inversion temperature to be 313.2 K. As anticipated, all curves intersect each other at the latter temperature, and characteristics concerning

the shape of the transition curve and the effect of N are all preserved as they have been discussed in Figure 3. A close inspection may reveal that the transition curves are asymmetric, especially at low N's, around the center of the RH $\alpha \rightarrow$ LH α transition. For example, the curve at $N = 100$ changes almost linearly with T on the coil side while remaining nearly flat on the helix side. This observation may allow a crude conjecture of the direction of the helix–coil transition.

IV. Concluding Remarks

In this study we have expanded the Zimm–Bragg–Nagai model[1,4,5] for the helix–coil transition to develop a theory applicable to the helix-sense inversion observed for poly(L-aspartate esters).[11] We have allowed each peptide residue to adopt three conformational states, i.e., RH α, LH α, and coil states, and have derived formal expressions for average fractions of helical conformers in terms of S, σ, and N. The key assumption in the present theory is that the conformational state of a given residue is influenced by those of neighboring residues. The hydrogen-bond formation and the side-chain nonbonded interaction are discussed as the factors responsible for this interaction, and it is shown that they exclude the occurrence of certain unfavorable sequences. Among excluded sequences those involving consecutive rl units are especially important, since their absences mean that the sense inversion proceeds accompanied by at least one coil residue between RH and LH α-helical sequences. In other words, the inversion is driven by a competition between tendencies to form RH and LH α-helices from coil residues. An ill-defined, molecular-order RH $\alpha \rightleftharpoons$ LH α equilibrium is thus reinterpreted in our model by the coexistence of two equilibria, RH $\alpha \rightleftharpoons$ coil and coil $\rightleftharpoons$ LH α, in the residual order.

In this paper we have restricted ourselves to establishing a model relevant to the sense inversion. Formulas are derived only for the conformer's fractions, although the theory can further be expanded to obtain other averages such as the length and the number of helical sequences. These quantities should be of importance in penetrating into the detailed mechanism of the sense inversion. An experimental determination of the $f_r - f_l$ vs. N relationship is also needed for a critical test of the theory. Nevertheless, even in the absence of these informations, fundamental aspects of the sense inversion can well be elucidated by the present model on the basis of calculated transition curves and their comparison with the previous observations for PPELA.[11]

Acknowledgment. The author thanks Professor A. Abe for critically reading the manuscript and valuable comments.

References and Notes

(1) Zimm, B. H.; Bragg, J. K. *J. Chem. Phys.* **1959**, *31*, 526.
(2) Gibbs, J. H.; DiMarzio, E. A. *J. Chem. Phys.* **1959**, *30*, 271.
(3) Miyake, A. *J. Polym. Sci.* **1960**, *46*, 169.
(4) Nagai, K. *J. Phys. Soc. Jpn.* **1960**, *15*, 407.
(5) Nagai, K. *J. Chem. Phys.* **1961**, *34*, 887.
(6) Lifson, S.; Roig, A. *J. Chem. Phys.* **1961**, *34*, 1963.
(7) Applequist, J. *J. Chem. Phys.* **1963**, *38*, 934.
(8) Zimm, B. H.; Doty, P.; Iso, K. *Proc. Natl. Acad. Sci. U.S.A.* **1959**, *45*, 1601.
(9) Okita, K.; Teramoto, A.; Fujita, H. *Biopolymers* **1970**, *9*, 717.
(10) Teramoto, A.; Norisuye, T.; Fujita, H. *Polym. J.* **1970**, *1*, 55.
(11) Toriumi, H.; Saso, N.; Yasumoto, Y.; Sasaki, S.; Uematsu, I. *Polym. J.* **1979**, *12*, 977.
(12) Bradbury, E. M.; Carpenter, B. G.; Goldman, H. *Biopolymers* **1968**, *6*, 837.
(13) Bradbury, E. M.; Carpenter, B. G.; Stephens, R. M. *Biopolymers* **1968**, *6*, 905.
(14) Bradbury, E. M.; Carpenter, B. G.; Robinson, C. C.; Goldman, H. *Macromolecules* **1971**, *4*, 557.
(15) Hashimoto, M.; Aritomi, J. *Bull. Chem. Soc. Jpn.* **1966**, *39*, 2707.
(16) Hashimoto, M.; Arakawa, S. *Bull. Chem. Soc. Jpn.* **1967**, *40*, 1698.
(17) Go, M.; Saito, N. *J. Phys. Soc. Jpn.* **1965**, *20*, 1686.
(18) Teramoto, A.; Fujita, H. *J. Macromol. Sci., Rev. Macromol. Chem.* **1976**, *C15*, 165.
(19) Hayashi, Y.; Teramoto, A.; Kawahara, K.; Fujita, H. *Biopolymers* **1969**, *8*, 403.

Mechanism of Thermal Degradation of Polyurethanes. Effect of Ammonium Polyphosphate

Giorgio Montaudo,*,† Concetto Puglisi,‡ Emilio Scamporrino,† and Daniele Vitalini‡

Istituto Dipartimentale di Chimica e Chimica Industriale, Università di Catania, 95125 Catania, Italy, and Istituto per la Chimica e la Tecnologia dei Materiali Polimerici, Consiglio Nazionale delle Ricerche, 95125 Catania, Italy. *Received July 18, 1983*

ABSTRACT: The thermal decomposition of some structurally related N–H and N-substituted polyurethanes and their mixtures with ammonium polyphosphate (APP) was investigated by thermogravimetry (TG) and direct pyrolysis in a mass spectrometer (MS). The N–H polyurethanes (I–III) undergo a quantitative depolymerization process with formation of compounds with amine and isocyanate end groups. On the other hand, the thermal degradation of the N-substituted polyurethanes (IV–IX) proceeds by a different mechanism as a function of their chemical structure. Three thermal degradation pathways have been ascertained: N–H hydrogen transfer (I–III), β-CH hydrogen transfer (IV–VII), and α-CH hydrogen transfer (V, VI, VIII, and IX). The addition of APP lowers the thermal stability of N-substituted polyurethanes V, VI, VIII, and IX, whereas that of the other polymers remains unaltered. Our data show that APP often changes the nature of the pyrolytic products, sometimes inducing a hydrolytic cleavage of the polymer chain and sometimes causing the formation of tertiary amines.

Introduction

Direct pyrolysis of polymers in the mass spectrometer (DP–MS) is an excellent method for monitoring the initial thermal fragmentation processes occurring when polymers are heated to decomposition.[1] We have investigated several classes of polymers by the DP–MS method[2–4,9] as a part of our longer term investigation of the primary thermal fragmentation processes of polycondensates.

Previous MS studies have shown that N–H substitution

† Università di Catania.
‡ Consiglio Nazionale delle Ricerche.

0024-9297/84/2217-1605$01.50/0